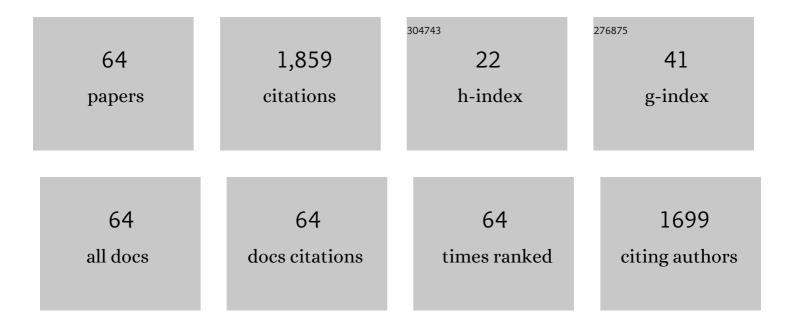
Peng-Wang Zhai

List of Publications by Year in descending order

Source: https://exaly.com/author-pdf/9429155/publications.pdf Version: 2024-02-01



DENC-WANC 7HAL

#	Article	IF	CITATIONS
1	Occurrence, liquid water content, and fraction of supercooled water clouds from combined CALIOP/IIR/MODIS measurements. Journal of Geophysical Research, 2010, 115, .	3.3	250
2	A vector radiative transfer model for coupled atmosphere and ocean systems with a rough interface. Journal of Quantitative Spectroscopy and Radiative Transfer, 2010, 111, 1025-1040.	2.3	129
3	A vector radiative transfer model for coupled atmosphere and ocean systems based on successive order of scattering method. Optics Express, 2009, 17, 2057.	3.4	116
4	Atmospheric Correction of Satellite Ocean-Color Imagery During the PACE Era. Frontiers in Earth Science, 2019, 7, .	1.8	98
5	Atmospheric correction for hyperspectral ocean color retrieval with application to the Hyperspectral Imager for the Coastal Ocean (HICO). Remote Sensing of Environment, 2018, 204, 60-75.	11.0	83
6	Going Beyond Standard Ocean Color Observations: Lidar and Polarimetry. Frontiers in Marine Science, 2019, 6, .	2.5	80
7	Joint retrieval of aerosol and water-leaving radiance from multispectral, multiangular and polarimetric measurements over ocean. Atmospheric Measurement Techniques, 2016, 9, 2877-2907.	3.1	69
8	Invisibility cloaks for irregular particles using coordinate transformations. Optics Express, 2008, 16, 6134.	3.4	55
9	Optical bistability in electromagnetically induced grating. Physics Letters, Section A: General, Atomic and Solid State Physics, 2001, 289, 27-33.	2.1	54
10	Electric and magnetic energy density distributions inside and outside dielectric particles illuminated by a plane electromagnetic wave. Optics Express, 2005, 13, 4554.	3.4	53
11	Impulse response solution to the three-dimensional vector radiative transfer equation in atmosphere-ocean systems I Monte Carlo method. Applied Optics, 2008, 47, 1037.	2.1	50
12	Integrating cavities: temporal response. Applied Optics, 2006, 45, 9053.	2.1	44
13	Cirrus optical depth and lidar ratio retrieval from combined CALIPSO loudSat observations using ocean surface echo. Journal of Geophysical Research, 2012, 117, .	3.3	44
14	Retrieval of aerosol properties and water-leaving reflectance from multi-angular polarimetric measurements over coastal waters. Optics Express, 2018, 26, 8968.	3.4	44
15	Modeling Atmosphere-Ocean Radiative Transfer: A PACE Mission Perspective. Frontiers in Earth Science, 2019, 7, .	1.8	37
16	Retrieving Aerosol Characteristics From the PACE Mission, Part 2: Multi-Angle and Polarimetry. Frontiers in Environmental Science, 2019, 7, .	3.3	37
17	Spectral sea surface reflectance of skylight. Optics Express, 2017, 25, A1.	3.4	34
18	Retrieving Aerosol Characteristics From the PACE Mission, Part 1: Ocean Color Instrument. Frontiers in Earth Science, 2019, 7, .	1.8	31

Peng-Wang Zhai

#	Article	IF	CITATIONS
19	Water-leaving contribution to polarized radiation field over ocean. Optics Express, 2017, 25, A689.	3.4	30
20	Efficient multi-angle polarimetric inversion of aerosols and ocean color powered by a deep neural network forward model. Atmospheric Measurement Techniques, 2021, 14, 4083-4110.	3.1	27
21	Inherent optical properties of the coccolithophore: Emiliania huxleyi. Optics Express, 2013, 21, 17625.	3.4	25
22	Vector radiative transfer model for coupled atmosphere and ocean systems including inelastic sources in ocean waters. Optics Express, 2017, 25, A223.	3.4	25
23	An optimization approach for aerosol retrievals using simulated MISR radiances. Atmospheric Research, 2012, 116, 1-14.	4.1	23
24	Equivalent path lengths in an integrating cavity: comment. Applied Optics, 2010, 49, 575.	2.1	22
25	CALIPSO lidar ratio retrieval over the ocean. Optics Express, 2011, 19, 18696.	3.4	22
26	Implementing the Near- to Far-Field Transformation in the Finite-Difference Time-Domain Method. Applied Optics, 2004, 43, 3738.	2.1	21
27	Effects of ice crystal surface roughness and air bubble inclusions on cirrus cloud radiative properties from remote sensing perspective. Journal of Quantitative Spectroscopy and Radiative Transfer, 2017, 195, 119-131.	2.3	21
28	Zero-backscatter cloak for aspherical particles using a generalized DDA formalism. Optics Express, 2008, 16, 2068.	3.4	19
29	Inversion of multiangular polarimetric measurements over open and coastal ocean waters: a joint retrieval algorithm for aerosol and water-leaving radiance properties. Atmospheric Measurement Techniques, 2019, 12, 3921-3941.	3.1	18
30	Lidar equation for ocean surface and subsurface. Optics Express, 2010, 18, 20862.	3.4	17
31	Inversion of multiangular polarimetric measurements from the ACEPOL campaign: an application of improving aerosol property and hyperspectral ocean color retrievals. Atmospheric Measurement Techniques, 2020, 13, 3939-3956.	3.1	17
32	Quantum-interference effects for gain leveling in optical fibers. Physical Review A, 2002, 65, .	2.5	16
33	Polarized radiance fields under a dynamic ocean surface: a three-dimensional radiative transfer solution. Applied Optics, 2009, 48, 3019.	2.1	16
34	Application of the symplectic finite-difference time-domain method to light scattering by small particles. Applied Optics, 2005, 44, 1650.	2.1	14
35	Contribution of Raman scattering to polarized radiation field in ocean waters. Optics Express, 2015, 23, 23582.	3.4	14
36	Testbed results for scalar and vector radiative transfer computations of light in atmosphere-ocean systems. Journal of Quantitative Spectroscopy and Radiative Transfer, 2020, 242, 106717.	2.3	14

Peng-Wang Zhai

#	Article	IF	CITATIONS
37	Impulse response solution to the three-dimensional vector radiative transfer equation in atmosphere-ocean systems II The hybrid matrix operatorMonte Carlo method. Applied Optics, 2008, 47, 1063.	2.1	13
38	Adaptive Data Screening for Multi-Angle Polarimetric Aerosol and Ocean Color Remote Sensing Accelerated by Deep Learning. Frontiers in Remote Sensing, 2021, 2, .	3.5	13
39	Advanced angular interpolation in the vector radiative transfer for coupled atmosphere and ocean systems. Journal of Quantitative Spectroscopy and Radiative Transfer, 2013, 115, 19-27.	2.3	12
40	Radiative Transfer Modeling of Phytoplankton Fluorescence Quenching Processes. Remote Sensing, 2018, 10, 1309.	4.0	12
41	Comment on the transmission matrix for a dielectric interface. Journal of Quantitative Spectroscopy and Radiative Transfer, 2012, 113, 1981-1984.	2.3	11
42	Uncertainty in the bidirectional reflectance model for oceanic waters. Applied Optics, 2015, 54, 4061.	2.1	11
43	FDTD far-field scattering amplitudes: Comparison of surface and volume integration methods. Journal of Quantitative Spectroscopy and Radiative Transfer, 2007, 106, 590-594.	2.3	10
44	Neural Network Reflectance Prediction Model for Both Open Ocean and Coastal Waters. Remote Sensing, 2020, 12, 1421.	4.0	10
45	Atmospheric correction over the ocean for hyperspectral radiometers using multi-angle polarimetric retrievals. Optics Express, 2021, 29, 4504.	3.4	10
46	An improved pseudo spherical shell algorithm for vector radiative transfer. Journal of Quantitative Spectroscopy and Radiative Transfer, 2022, 282, 108132.	2.3	10
47	Uncertainty and interpretation of aerosol remote sensing due to vertical inhomogeneity. Journal of Quantitative Spectroscopy and Radiative Transfer, 2013, 114, 91-100.	2.3	9
48	Single scattering properties of non-spherical hydrosols modeled by spheroids. Optics Express, 2018, 26, A124.	3.4	8
49	Mueller matrix imaging of targets under an air-sea interface. Applied Optics, 2009, 48, 250.	2.1	7
50	Platform effects on optical variability and prediction of underwater visibility. Applied Optics, 2010, 49, 2784.	2.1	7
51	Cloud remote sensing with EPIC/DSCOVR observations: A sensitivity study with radiative transfer simulations. Journal of Quantitative Spectroscopy and Radiative Transfer, 2019, 230, 56-60.	2.3	7
52	Cloud detectionÂoverÂsnow and iceÂwith oxygen A- and B-band observations from the Earth Polychromatic Imaging Camera (EPIC). Atmospheric Measurement Techniques, 2020, 13, 1575-1591.	3.1	7
53	Analysis of Water Vapor Correction for CloudSat W-Band Radar. IEEE Transactions on Geoscience and Remote Sensing, 2013, 51, 3812-3825.	6.3	5
54	A Radiative Transfer Simulator for PACE: Theory and Applications. Frontiers in Remote Sensing, 2022, 3,	3.5	5

PENG-WANG ZHAI

#	Article	IF	CITATIONS
55	FDTD solutions for the distribution of radiation from dipoles embedded in dielectric particles. Journal of Quantitative Spectroscopy and Radiative Transfer, 2007, 106, 257-261.	2.3	4
56	Exact first order scattering correction for vector radiative transfer in coupled atmosphere and ocean systems. , 2012, , .		4
57	Cloud Detection Over Sunglint Regions With Observations From the Earth Polychromatic Imaging Camera. Frontiers in Remote Sensing, 2021, 2, .	3.5	4
58	Decoupling error for the atmospheric correction in ocean color remote sensing algorithms. Journal of Quantitative Spectroscopy and Radiative Transfer, 2010, 111, 1958-1963.	2.3	3
59	Equivalence of internal and external mixture schemes of single scattering properties in vector radiative transfer. Applied Optics, 2017, 56, 4105.	2.1	3
60	Monostatic lidar/radar invisibility using coated spheres. Optics Express, 2008, 16, 1431.	3.4	2
61	Augmenting Heritage Ocean-Color Aerosol Models for Enhanced Remote Sensing of Inland and Nearshore Coastal Waters. Frontiers in Remote Sensing, 2022, 3, .	3.5	2
62	The far-field modified uncorrelated single-scattering approximation in light scattering by a small volume element. Optics Express, 2007, 15, 8479.	3.4	1
63	Optical gain and grating structure in the collective atomic recoil laser. Physics Letters, Section A: General, Atomic and Solid State Physics, 1999, 254, 251-256.	2.1	0
64	Aerosol properties from combined oxygen A band radiances and lidar. , 2015, , .		0